

Supplemental Information:

Increasing the Weights in the Molecular Work-out of *cis*- and *trans*-Formic Acid: Extension of the Vibrational Data Base *via* Deuteriation

Arman Nejad, Martin A. Suhm and Katharina A. E. Meyer*

Institute of Physical Chemistry, University of Göttingen, Tammannstr. 6, 37077 Göttingen (Germany). E-mail: katharina.meyer@chemie.uni-goettingen.de

Contents

1 Methods	S2
1.1 Experimental details	S2
1.2 Computational details	S2
2 Formic acid fundamentals	S4
3 Spectra of <i>cis</i>-formic acid	S6
References	S10

List of Tables

S1 Details about used chemicals	S2
S2 Keywords used in quantum chemical calculations	S2
S3 Harmonic IR/Raman intensities at B3LYP-D3(BJ)/aVTZ	S4
S4 Comparison of Raman band positions	S4

List of Figures

S1 Harmonically avoided crossings of <i>trans</i> -formic acid fundamentals	S5
S2 O–H/D stretching (ν_1) spectra of <i>cis</i> -formic acid	S6
S3 C–H/D stretching (ν_2) spectra of <i>cis</i> -formic acid	S7
S4 C=O stretching (ν_3) spectra of <i>cis</i> -formic acid	S8
S5 O–D bending (ν_5) spectra of <i>cis</i> -formic acid	S9

1 Methods

1.1 Experimental details

H/D exchange and impurities

Isotopic H/D impurities in the spectra were assessed by comparison of integrated intensities of suitable vibrational bands and computed harmonic Raman scattering cross-section ratios as

$$\frac{N_1}{N_2} = \frac{\sigma_2}{\sigma_1} \cdot \frac{\int I_1(\tilde{\nu}) d\tilde{\nu}}{\int I_2(\tilde{\nu}) d\tilde{\nu}}.$$

For integrated intensities, we assign error bars of $\pm 20\%$ and calculate resulting impurity errors using the Gaussian error propagation. The acidic H/D exchange for HCOOD was estimated analysing the ν_6 and ν_1 spectral regions, where vibrational bands of HCOOH and HCOOD can be found in the same spectral window. The same applies to DCOOH impurities in DCOOD spectra. Detailed analysis and comparison of respective spectral regions of all H/D isotopologues further revealed DCOOD impurities in all recorded spectra of DCOOH, which are nearly twice as high as the acidic H/D impurities in spectra of HCOOD/DCOOH. Therefore, it seems likely that these are partly due to the manufacturing process.

Table S1: Detailed information about all H/D isotopologues of formic acid are listed alongside an estimated upper bound of the formic acid concentrations in the helium expansion and observed isotopologic impurities.

Chemical	Lot#	Manufacturer	Concentration in He	Impurities
HCOOH	A0380211	Acros Organics, 98+%	< 0.2%	-
DCOOH	1401769	abcr, 95 wt% in H ₂ O; 98 atom%D	< 0.4%	(6 \pm 2)% DCOOD
HCOOD	PR-19516/07238FA1	Cambridge Isotope Laboratories, Inc. (OD, 98%) (<5% D ₂ O)	< 0.4%	(3 \pm 1)% HCOOH
HCOOD	1424534	abcr, 95 wt% in D ₂ O; 98 atom%D	< 0.3%	(3 \pm 1)% HCOOH
DCOOD	1414704	abcr, 95 wt% in D ₂ O; 98 atom%D	< 0.2 – 0.4%	(2 \pm 1)% DCOOH

1.2 Computational details

Geometry optimisation and harmonic frequencies

Geometry optimisation and harmonic vibrational frequency calculations at the CCSD(T)^[1] level have been performed with CFOUR version 1.^[2, 3] Geometry optimisation, harmonic frequency, (harmonic) IR, and Raman activity calculations at all other levels have been carried out with GAUSSIAN 09 Rev. E.01.^[4] All specified input parameters are summarised in Tab. S2. Raman scattering cross-sections have been computed according to Eq. 1 (main text) and are shown in Tab. S3 at the B3LYP-D3(BJ)/aVTZ level.

Table S2: Keywords which have been specified in GAUSSIAN 09 Rev. E.01^[4] and CFOUR version 1^[2, 3] calculations using Dunning's correlation consistent aug-cc-pVTZ^[5] (aVTZ) basis set.

Method	Program	Symmetry	Keywords
HF, MP2	GAUSSIAN	on	Opt=VeryTight Freq=Raman
B3LYP, PBE0 B2PLYP	GAUSSIAN	on	EmpiricalDispersion=GD3BJ DenFit Integral(Grid=SuperFineGrid) Opt=VeryTight Freq=Raman
CCSD(T)	CFOUR	on	FROZEN_CORE=ON SCF_CONV=10 CC_CONV=10 CC_PROGRAM=ECC VIB=EXACT ABCDTYPE=AOBASIS LINEQ_CONV=10 GEO_CONV=10 GEO_METHOD=NR

Quartic force field and Fermi resonance constant W

Expanding the PES as a Taylor series up to fourth order in dimensionless normal coordinates \mathbf{q} around the equilibrium, one obtains

$$\frac{V(\mathbf{q})}{hc} = \sum_k \omega_k q_k^2 + \frac{1}{3!} \sum_{klm} \phi_{klm} q_k q_l q_m + \frac{1}{4!} \sum_{klmn} \phi_{klmn} q_k q_l q_m q_n, \quad (1)$$

where ϕ are the derivatives of the potential energy with respect to dimensionless normal coordinates (using a non-restrictive summation) and ω the harmonic frequencies. From the available formic acid PES (with analytical Hessians) fortran routine by Tew and Mizukami,^[6] the quartic force field (QFF) was obtained by two-step numerical differentiation in normal coordinates using the PyPES program package^[7] with default settings and the following reference geometries:

```
5
Equilibrium geometry of trans-formic acid in bohr
C 0.7813670998 0.0000000000 0.1870289330
H 2.8443983303 0.0000000000 0.0625424285
O -0.4067012605 0.0000000000 2.1159295718
O -0.2299101242 0.0000000000 -2.1389130948
H -2.0445178745 0.0000000000 -1.9246987056
```

```
5
Equilibrium geometry of cis-formic acid in bohr
C 0.7563063927 0.0000000000 0.1917690324
H 2.8307835834 0.0000000000 0.0574837406
O -0.3789085156 0.0000000000 2.1376897827
O -0.4190401473 0.0000000000 -2.0713552046
H 0.8280301033 0.0000000000 -3.3936226467
```

From the cubic force constants ϕ , model off-diagonal matrix elements W are obtained by scaling them with appropriate factors^[8] for Fermi type 1 ($\omega_i \approx 2\omega_j$)

$$W_{ijj} = \frac{\phi_{ijj}}{4} \quad (2)$$

and type 2 resonances ($\omega_i \approx \omega_j + \omega_k$)

$$W_{ijk} = \frac{\phi_{ijk}}{\sqrt{8}}. \quad (3)$$

2 Formic acid fundamentals

Table S3: Harmonic wavenumbers (ω , in cm^{-1}), IR oscillator strengths (S_{IR} , in km mol^{-1}), and Raman scattering cross-sections (σ_{Ra} , in $10^{-36} \text{ m}^2 \text{ sr}^{-1}$) for all four H/D isotopologues of *cis*- and *trans*-formic acid, computed at the B3LYP-D3(BJ)/aVTZ level.

			ν_1	ν_2	ν_3	ν_4	ν_5	ν_6	ν_7	ν_8	ν_9
HCOOH	<i>trans</i>	ω	3716.5	3048.7	1811.4	1401.9	1298.7	1121.6	629.1	1051.6	674.6
		S_{IR}	60.5	39.7	372.9	2.4	9.0	262.1	41.6	2.0	137.2
		σ_{Ra}	76.1	171.8	39.7	19.2	9.9	12.5	34.5	6.1	4.4
	<i>cis</i>	ω	3781.5	2962.5	1856.2	1414.1	1269.0	1104.5	659.9	1032.5	530.5
		S_{IR}	59.0	73.7	309.9	0.4	309.4	57.5	9.4	0.0	82.7
		σ_{Ra}	104.4	172.2	47.5	14.9	8.2	50.8	4.1	7.4	9.7
DCOOH	<i>trans</i>	ω	3716.3	2267.2	1779.0	984.9	1294.9	1157.5	623.2	885.8	664.0
		S_{IR}	61.4	58.0	367.2	50.0	0.6	200.7	42.0	1.3	132.1
		σ_{Ra}	78.4	124.3	56.0	9.9	12.2	20.3	32.8	1.4	5.4
	<i>cis</i>	ω	3781.4	2206.2	1819.3	988.9	1263.1	1147.9	653.3	876.3	525.5
		S_{IR}	59.2	93.3	291.5	11.8	274.8	61.3	8.7	1.0	91.3
		σ_{Ra}	104.0	117.8	70.6	31.1	11.1	31.3	3.9	1.6	10.9
HCOOD	<i>trans</i>	ω	2702.1	3049.3	1805.5	1392.6	999.0	1186.4	561.6	1049.4	530.5
		S_{IR}	40.0	35.9	355.5	2.6	72.1	170.3	41.9	0.5	84.7
		σ_{Ra}	75.9	160.9	39.2	17.0	6.7	18.6	31.1	6.9	1.4
	<i>cis</i>	ω	2752.8	2962.5	1849.8	1412.9	913.9	1171.0	630.5	1032.5	399.0
		S_{IR}	38.2	71.4	335.3	1.6	6.3	290.9	9.8	0.0	30.7
		σ_{Ra}	85.8	175.9	49.6	14.4	37.8	16.6	1.8	7.4	3.2
DCOOD	<i>trans</i>	ω	2702.7	2266.0	1775.1	1049.6	959.9	1179.9	557.6	885.7	512.8
		S_{IR}	36.3	57.4	351.6	5.3	58.5	158.9	41.9	1.7	77.6
		σ_{Ra}	65.3	126.6	54.8	12.5	7.2	23.3	29.8	1.5	0.8
	<i>cis</i>	ω	2753.0	2204.8	1814.6	1045.6	891.4	1172.7	623.2	875.9	393.2
		S_{IR}	36.3	92.2	316.6	37.7	2.9	239.8	9.1	1.7	37.2
		σ_{Ra}	89.5	118.6	71.4	14.1	38.2	16.1	1.9	1.7	2.9

Table S4: Comparison of Raman jet (this work) and Raman gas phase band positions (Bertie *et al.*^[9, 10]) for *trans*-formic acid. Differences in nomenclature employed by Bertie *et al.* (Herzberg nomenclature for each isotopologue) and this work (Herzberg nomenclature for HCOOH applied to all isotopologues) are highlighted in red. All reported values are in units of cm^{-1} . Fermi resonance doublets are indicated by braces.

HCOOH		DCOOH		HCOOD		DCOOD	
This work	Bertie <i>et al.</i>	This work	Bertie <i>et al.</i>	This work	Bertie <i>et al.</i>	This work	Bertie <i>et al.</i>
<i>trans</i>							
ν_1	$\left\{ 3570 \quad 3568.9 \atop 3567 \right\}$	ν_1	$3569 \quad 3566$	ν_1	$2631 \quad 2631.4$	ν_2	$2632 \quad 2631.9$
ν_2	$2942 \quad 2942.0$	ν_2	$2219 \quad 2218$	ν_2	$\left\{ 2954 \atop 2938 \quad 2938.2^b \right\}$	ν_1	$\left\{ 2231 \quad 2231.8 \atop 2194 \quad 2195.1 \right\}$
ν_3	$1776 \quad 1776.6$	ν_3	$\left\{ 1762 \quad 1760 \atop 1725 \quad 1724 \right\}$	ν_3	$1772 \quad 1773$	ν_3	$\left\{ 1761 \quad 1760.0 \atop 1725 \quad 1723.5 \right\}$
ν_4	$1379 \quad 1380.6$	ν_4	971	ν_4	$1365 \quad 1368$	ν_4	$1039 \quad 1042$
$2\nu_9$	$\left\{ 1306 \quad 1307.1^a \atop 1220 \right\}$	ν_5	$\left\{ 1299 \quad 1297 \atop 1206 \right\}$	ν_4	$\left\{ 972 \quad 972^c \atop 1010 \right\}$	ν_6	$945 \quad 945.0$
ν_6	$1104 \quad 1103.8$	ν_6	$1142 \quad 1140$	ν_5	$1176 \quad 1177.9$	ν_5	$1170 \quad 1169.7$
ν_7	$626 \quad 624.9$	ν_7	$620 \quad 620$	ν_7	$558 \quad 560.2$	ν_7	$554 \quad 555.5$
ν_8		ν_8		ν_8		ν_8	
ν_9	642	ν_9	ν_9	ν_9	ν_9	ν_9	ν_9

^a Originally assigned to $2\nu_9$ by Bertie *et al.*

^b Bertie *et al.* originally assigned a Fermi resonance doublet at 2941.8 and 2938.2 to $\nu_1/\nu_3 + \nu_6$. The band at 2941.8 is most likely ν_2 of *trans*-HCOOH.

^c Tentative assignment by Bertie *et al.*

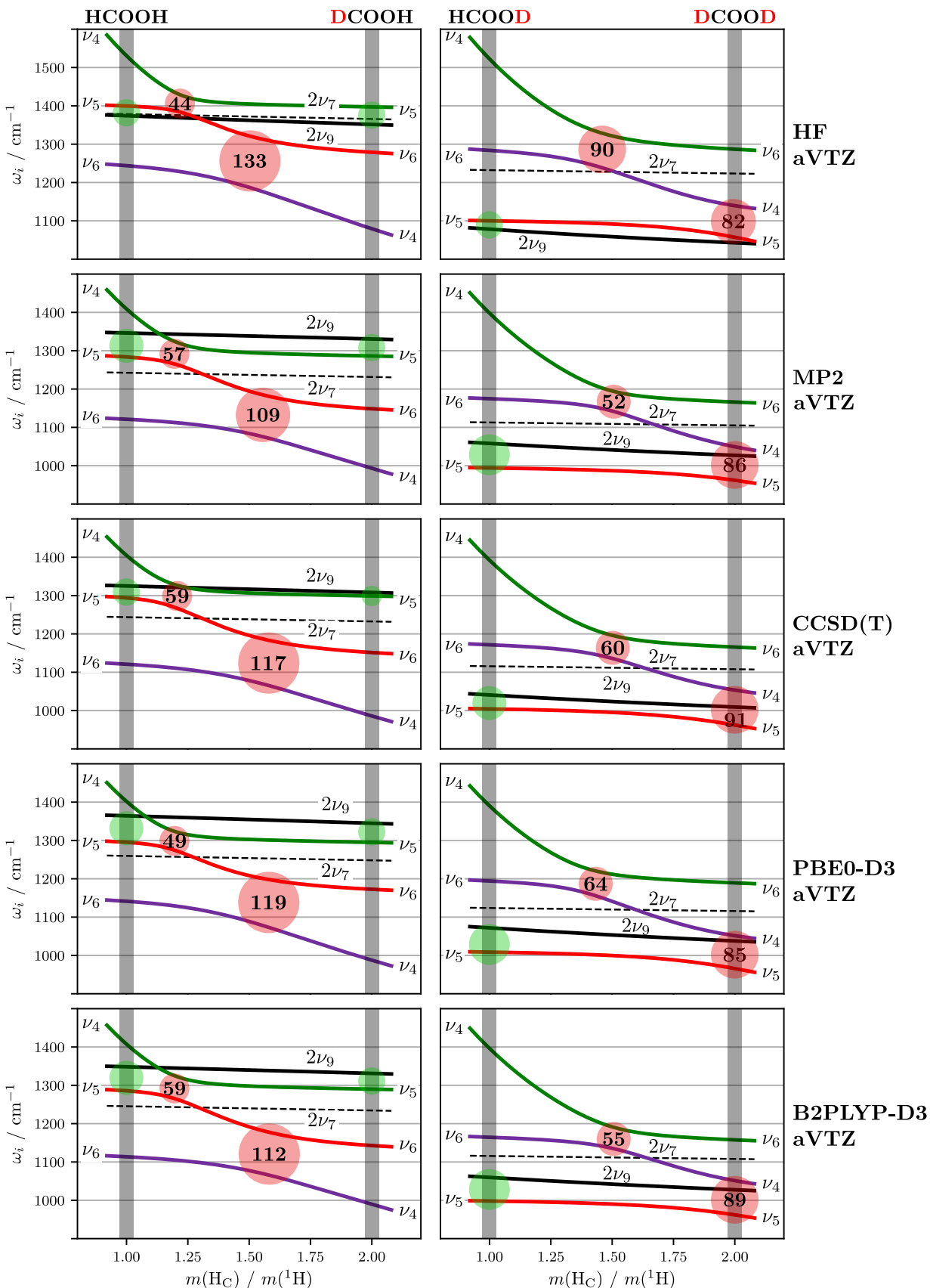


Figure S1: Harmonic wavenumbers (in cm^{-1}) of A' symmetric fundamentals and overtones in the spectral windows between 900 and 1600 cm^{-1} as a function of the relative C–H proton mass of *trans*-formic acid (left O–H, right O–D). This figure is the same as Fig. 6 in the main manuscript, showing other electronic structure methods than B3LYP-D3. Grey bars indicate fractional masses which equal the mass of hydrogen or deuterium. Harmonically avoided crossings due to mode-mixing are indicated by a red disk in the interaction region, in which twice the effective coupling constant $2W$ is printed in bold letters. Green disks highlight the Fermi resonance-coupled states ν_5 and $2\nu_9$ in *trans*-HCOOH, -DCOOH, and -HCOOD.

3 Spectra of *cis*-formic acid

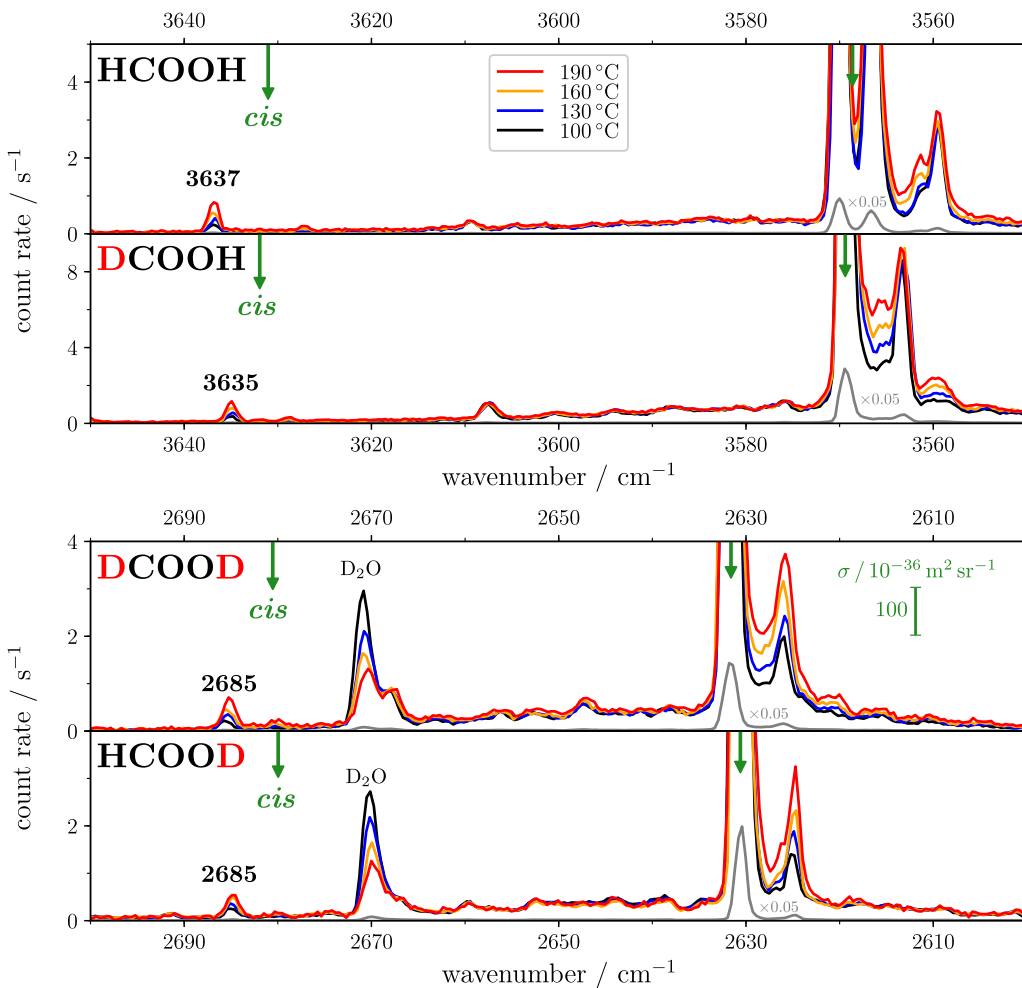


Figure S2: Raman jet spectra of the four H/D isotopologues of formic acid in the O–H (top) and O–D (bottom) stretching region (ν_1) with increasing nozzle temperature. For each isotopologue, the spectra have been intensity-scaled to the ν_1 band of *trans*-formic acid with the lowest intensity amongst the four temperatures. For an overview of the overall spectral intensity, the 160 °C spectrum is additionally shown further intensity-scaled ($\times 0.05$) in grey. The band position (in cm^{-1}) is shown for the ν_1 fundamentals of the respective *cis*-conformers. For each isotopologue, harmonic $\nu_1(\text{trans})$ -scaled line positions (calculated at the B3LYP-D3(BJ)/aVTZ level) are shown in green using scaling factors of 0.960, 0.960, 0.974, and 0.974 (top to bottom). In case of Fermi resonance-doubling, as observed for HCOOH, the resonance band centre is used as a scaling reference.

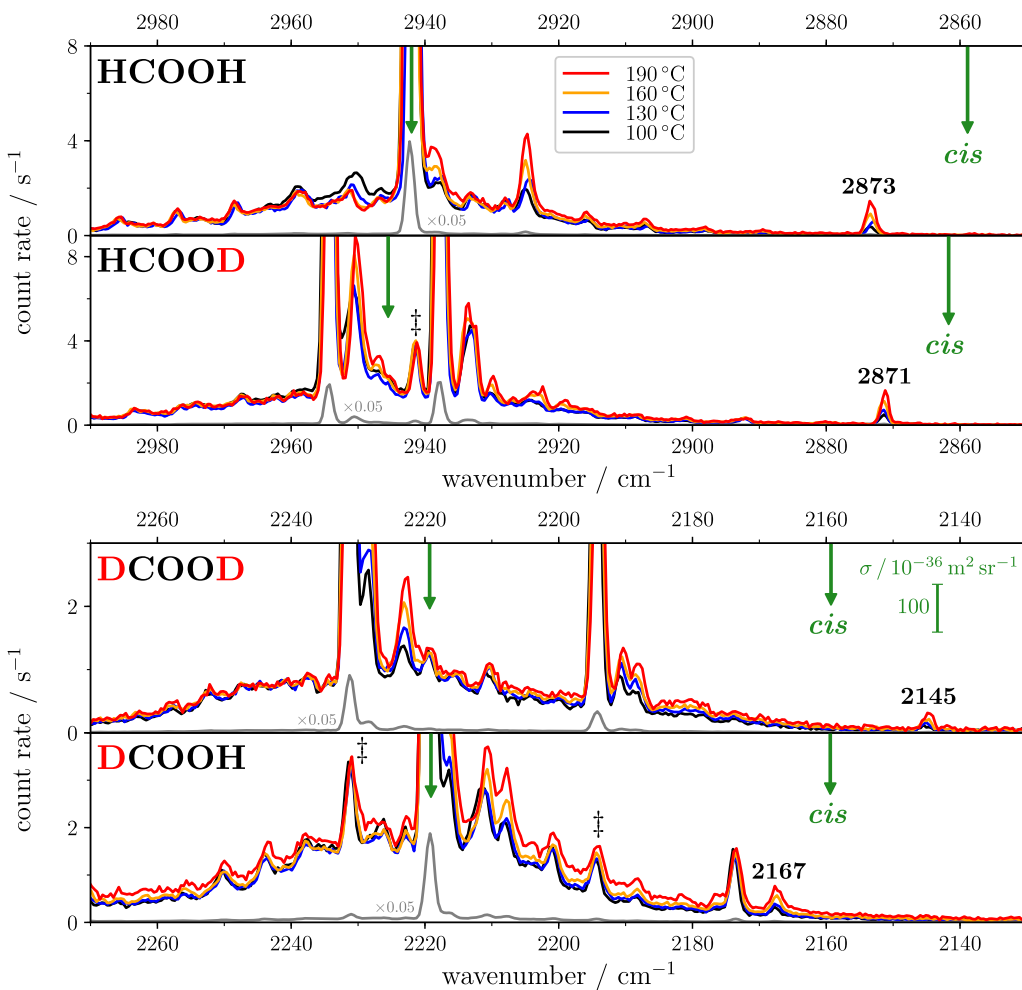


Figure S3: Raman jet spectra of the four H/D isotopologues of formic acid in the C–H (top) and C–D (bottom) stretching region (ν_2) with increasing nozzle temperature. For each isotopologue, the spectra have been intensity-scaled to the ν_2 band of *trans*-formic acid with the lowest intensity amongst the four temperatures. For an overview of the overall spectral intensity, the 160 °C spectrum is additionally shown further intensity-scaled ($\times 0.05$) in grey. The band position (in cm⁻¹) is shown for the ν_2 fundamentals of the respective *cis*-conformers. For each isotopologue, harmonic ν_2 (*trans*)-scaled line positions (calculated at the B3LYP-D3(BJ)/aVTZ level) are shown in green using scaling factors of 0.965, 0.966, 0.979, and 0.979 (top to bottom). In case of Fermi resonance-doubling, as observed for HCOOD and DCOOD, the resonance band centre is used as a scaling reference. Bands of isotopic impurities are labelled as ‡.

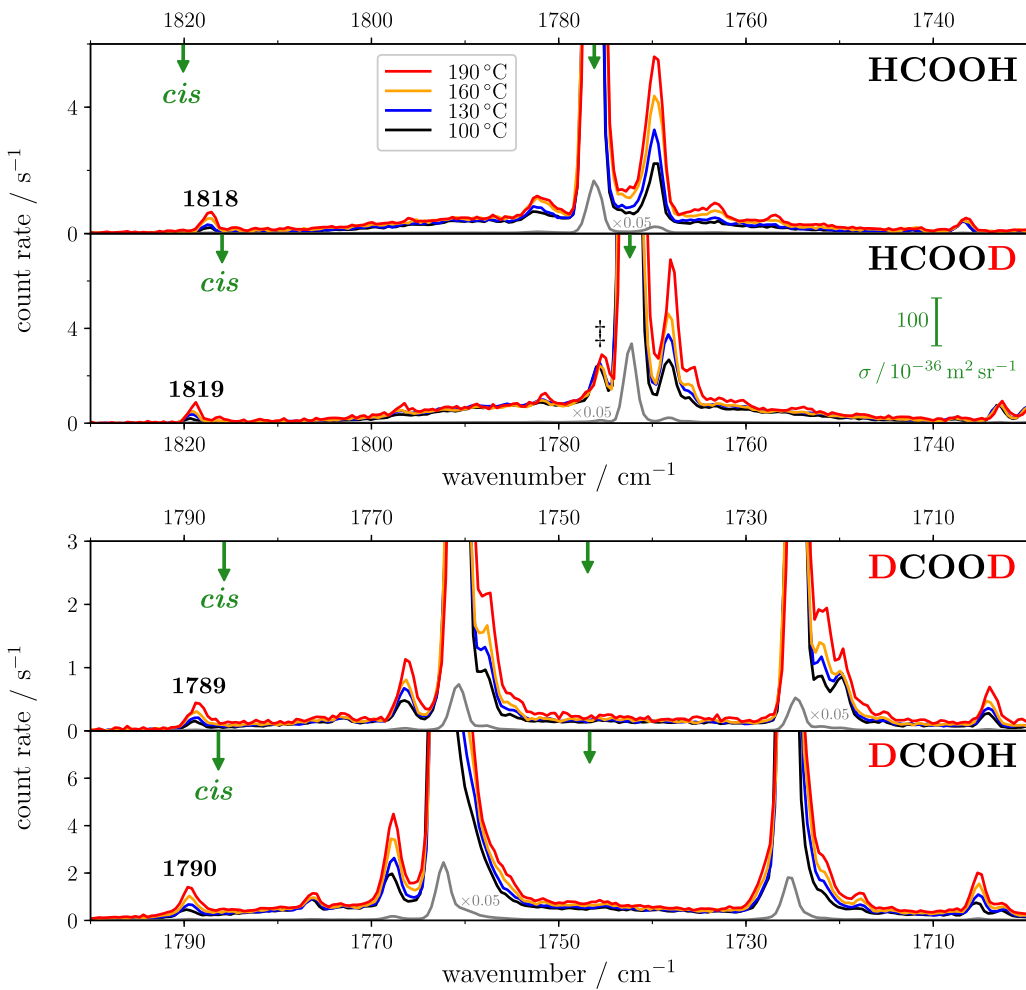


Figure S4: Raman jet spectra of the four H/D isotopologues of formic acid in the C=O stretching region (ν_3) with increasing nozzle temperature for C-hydrogenated (top) and C-deuterated (bottom) formic acids. For each isotopologue, the spectra have been intensity-scaled to the ν_3 band of *trans*-formic acid with the lowest intensity amongst the four temperatures. For an overview of the overall spectral intensity, the 160 °C spectrum is additionally shown further intensity-scaled ($\times 0.05$) in grey. The band position (in cm^{-1}) is shown for the ν_3 fundamentals of the respective *cis*-conformers. For each isotopologue, harmonic $\nu_3(\text{trans})$ -scaled line positions (calculated at the B3LYP-D3(BJ)/aVTZ level) are shown in green using scaling factors of 0.981, 0.982, 0.984, and 0.982 (top to bottom). In case of Fermi resonance-doubling, as observed for DCOOH and DCOOD, the resonance band centre is used as a scaling reference. Bands of isotopic impurities are labelled as ‡.

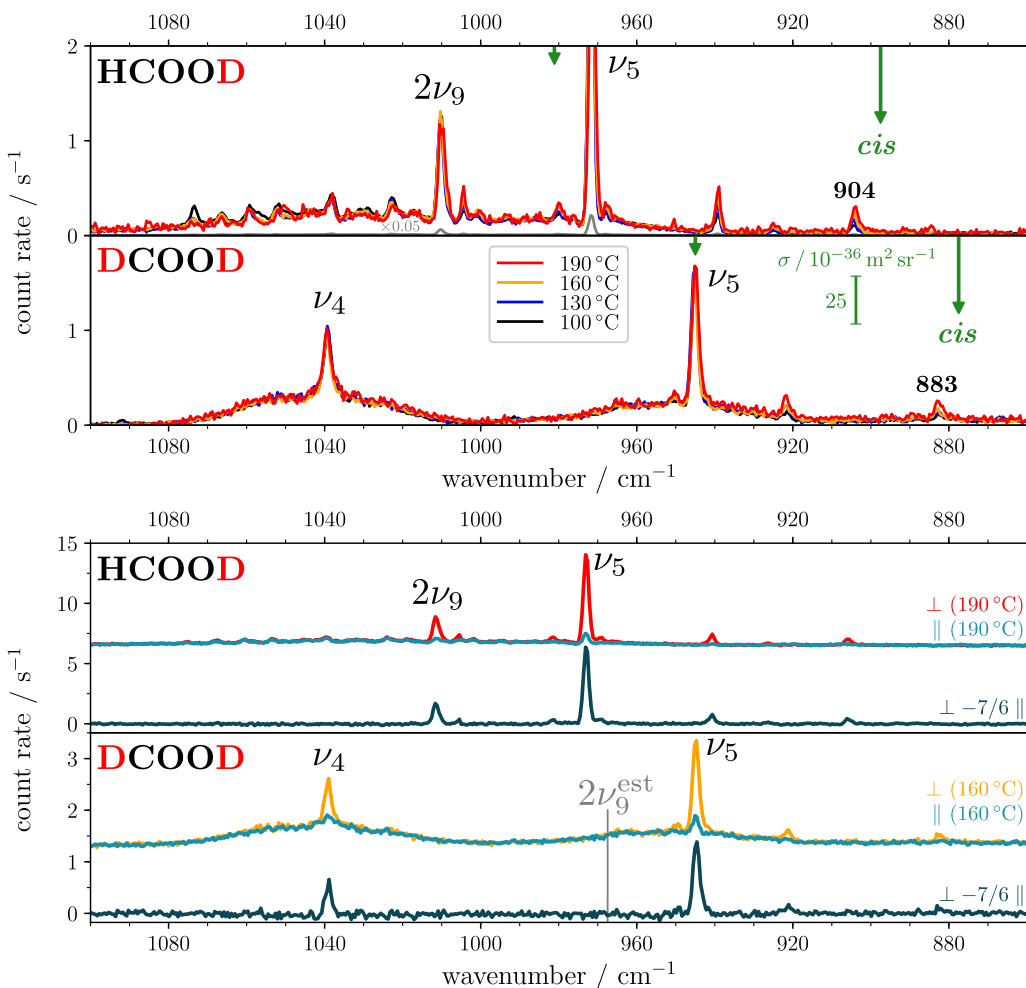


Figure S5: (top) Raman jet spectra of the O–D bending region (ν_5) with increasing nozzle temperature. For each isotopologue, the spectra have been intensity-scaled to the ν_6 band (not shown) of *trans*-formic acid with the lowest intensity amongst the four temperatures. For an overview of the overall spectral intensity, the 160 °C spectrum of HCOOD is additionally shown further intensity-scaled ($\times 0.05$) in grey. The band position (in cm^{-1}) is shown for the ν_5 fundamentals of the respective *cis*-conformers. For each isotopologue, harmonic ν_5 (*trans*)-scaled line positions (calculated at the B3LYP-D3(BJ)/aVTZ level) are shown in green using scaling factors of 0.982 and 0.984 for HCOOD and DCOOD, respectively. In case of Fermi resonance-doubling, as observed for HCOOD, the resonance band centre is used as a scaling reference. (bottom) Raman jet spectra of the O–D bending region (ν_5) with the polarisation of the incident laser (operated at 20 W) perpendicular (\perp , default for all other measurements) and parallel (\parallel) with respect to the scattering plane,^[11] and residual after subtraction ($\perp -7/6 \parallel$).^[12] Bands with smaller depolarisation ratios persist more in the residual spectrum. The band position of $2\nu_9$ has been estimated for DCOOD, see caption to Figure 4 for further details.

References

- [1] J. Gauss, J. F. Stanton, *Chem. Phys. Lett.* **1997**, *276*, 70–77.
- [2] J. F. Stanton, J. Gauss, L. Cheng, M. E. Harding, D. A. Matthews, P. G. Szalay, CFOUR, Coupled-Cluster techniques for Computational Chemistry, a quantum-chemical program package, With contributions from A.A. Auer, R.J. Bartlett, U. Benedikt, C. Berger, D.E. Bernholdt, Y.J. Bomble, O. Christiansen, F. Engel, R. Faber, M. Heckert, O. Heun, M. Hilgenberg, C. Huber, T.-C. Jagau, D. Jonsson, J. Jusélius, T. Kirsch, K. Klein, W.J. Lauderdale, F. Lipparini, T. Metzroth, L.A. Mück, D.P. O'Neill, D.R. Price, E. Prochnow, C. Puzzarini, K. Ruud, F. Schiffmann, W. Schwalbach, C. Simmons, S. Stopkowicz, A. Tajti, J. Vázquez, F. Wang, J.D. Watts and the integral packages MOLECULE (J. Almlöf and P.R. Taylor), PROPS (P.R. Taylor), ABACUS (T. Helgaker, H.J. Aa. Jensen, P. Jørgensen, and J. Olsen), and ECP routines by A. V. Mitin and C. van Wüllen. For the current version, see <http://www.cfour.de>.
- [3] D. A. Matthews, L. Cheng, M. E. Harding, F. Lipparini, S. Stopkowicz, T.-C. Jagau, P. G. Szalay, J. Gauss, J. F. Stanton, *J. Chem. Phys.* **2020**, *152*, 214108.

- [4] M. J. Frisch, G. W. Trucks, H. B. Schlegel, G. E. Scuseria, M. A. Robb, J. R. Cheeseman, G. Scalmani, V. Barone, B. Mennucci, G. A. Petersson, H. Nakatsuji, M. Caricato, X. Li, H. P. Hratchian, A. F. Izmaylov, J. Bloino, G. Zheng, J. L. Sonnenberg, M. Hada, M. Ehara, K. Toyota, R. Fukuda, J. Hasegawa, M. Ishida, T. Nakajima, Y. Honda, O. Kitao, H. Nakai, T. Vreven, Montgomery, J. A., Jr., J. E. Peralta, F. Ogliaro, M. Bearpark, J. J. Heyd, E. Brothers, K. N. Kudin, V. N. Staroverov, R. Kobayashi, J. Normand, K. Raghavachari, A. Rendell, J. C. Burant, S. S. Iyengar, J. Tomasi, M. Cossi, N. Rega, J. M. Millam, M. Klene, J. E. Knox, J. B. Cross, V. Bakken, C. Adamo, J. Jaramillo, R. Gomperts, R. E. Stratmann, O. Yazyev, A. J. Austin, R. Cammi, C. Pomelli, J. W. Ochterski, R. L. Martin, K. Morokuma, V. G. Zakrzewski, G. A. Voth, P. Salvador, J. J. Dannenberg, S. Dapprich, A. D. Daniels, Ö. Farkas, J. B. Foresman, J. V. Ortiz, J. Cioslowski, D. J. Fox, Gaussian 09 Revision E.01, Gaussian Inc. Wallingford CT, **2009**.
- [5] T. H. Dunning Jr., *J. Chem. Phys.* **1989**, *90*, 1007–1023.
- [6] D. P. Tew, W. Mizukami, *J. Phys. Chem. A* **2016**, *120*, 9815–9828.
- [7] M. Sibaev, D. L. Crittenden, *J. Chem. Phys.* **2016**, *144*, 214107.
- [8] J. M. L. Martin, T. J. Lee, P. R. Taylor, J. François, *J. Chem. Phys.* **1995**, *103*, 2589–2602.
- [9] J. E. Bertie, K. H. Michaelian, *J. Chem. Phys.* **1982**, *76*, 886–894.
- [10] J. E. Bertie, K. H. Michaelian, H. H. Eysel, D. Hager, *J. Chem. Phys.* **1986**, *85*, 4779–4789.
- [11] T. Forsting, M. A. Suhm, **2019**, see <https://doi.org/10.6084/m9.figshare.6395840.v1>.
- [12] D. A. Long, *The Raman effect: A unified treatment of the theory of Raman scattering by molecules*, Wiley, Chichester and New York, **2002**.